nature computational science

Article

https://doi.org/10.1038/s43588-024-00621-8

Strategy evolution on higher-order networks

Received: 7 November 2023

Accepted: 12 March 2024

Published online: 15 April 2024

Check for updates

Anzhi Sheng [1,2], Qi Su [3,4,5] ✉, Long Wang [1,6] ✉ & Joshua B. Plotkin [2,7] ✉

Cooperation is key to prosperity in human societies. Population structure is well understood as a catalyst for cooperation, where research has focused on pairwise interactions. But cooperative behaviors are not simply dyadic, and they often involve coordinated behavior in larger groups. Here we develop a framework to study the evolution of behavioral strategies in higher-order population structures, which include pairwise and multi-way interactions. We provide an analytical treatment of when cooperation will be favored by higher-order interactions, accounting for arbitrary spatial heterogeneity and nonlinear rewards for cooperation in larger groups. Our results indicate that higher-order interactions can act to promote the evolution of cooperation across a broad range of networks, in public goods games. Higher-order interactions consistently provide an advantage for cooperation when interaction hyper-networks feature multiple conjoined communities. Our analysis provides a systematic account of how higher-order interactions modulate the evolution of prosocial traits.

Humans rely on collective cooperation for social prosperity and even survival, whether tackling the spread of infectious diseases[1], combating climate change[2] or stabilizing ecosystems[3]. The emergence of prosocial behaviors that benefit others at a cost to oneself remains a topic of active study in evolutionary theory[4]. Population structure constrains the range of interactions while a trait spreads, which is known to facilitate prosocial traits by increasing the chance of phenotypic assortment and mutual cooperation. Network models offer a way to formalize population structure, where nodes represent individuals and edges denote pairwise social interactions between connected nodes. Both Monte Carlo simulations and mathematical models of strategic interactions and behavioral spread on networks have shown that population structure can play an important role in catalyzing cooperation[5–16]. Some of these studies[9] make explicit connections to the larger literature in theoretical population genetics[17,18].

But cooperation is not only a dyadic phenomenon. Pairwise interactions, or even the aggregation of many pairwise interactions, do not capture the nature of many forms of collective social behavior in human societies. Real-world interactions may involve more than two individuals simultaneously[19–27], and they are better described as a broad class of multiplayer cooperative dilemmas[28,29]. For instance, academic collaboration often involves many authors or research institutions, and the value of a paper is not simply the sum of each author's contribution, or their pairwise effects. In ecological communities more generally, the interaction between two individuals may be promoted or inhibited by the simultaneous behavior of a third individual, and these effects may not be represented as the aggregation of pairwise effects[30]. Social events involving multiple participants inherently unfold in groups[31]. Other examples include information spread on networks[32], group formation[33] and system synchronization[34]. These forms of social interaction that involve multiple simultaneous agents and have nonlinear effects in individuals' behavior are referred to as 'higher-order' interactions.

Recent studies in fields outside of evolution have found that higher-order interactions can have a significant impact on system dynamics, and even reverse outcomes that arise under strictly pairwise interactions. For instance, when the relationship between species is competitive, higher-order interactions can stabilize dynamics, while strictly pairwise interactions produce oscillations[35]. In the context of social contagion, a sufficiently high infectivity rate for higher-order

[1]Center for Systems and Control, College of Engineering, Peking University, Beijing, China. [2]Department of Biology, University of Pennsylvania, Philadelphia, PA, USA. [3]Department of Automation, Shanghai Jiao Tong University, Shanghai, China. [4]Key Laboratory of System Control and Information Processing, Ministry of Education of China, Shanghai, China. [5]Shanghai Engineering Research Center of Intelligent Control and Management, Shanghai, China. [6]Center for Multi-Agent Research, Institute for Artificial Intelligence, Peking University, Beijing, China. [7]Center for Mathematical Biology, University of Pennsylvania, Philadelphia, PA, USA. ✉e-mail: qisu@sjtu.edu.cn; longwang@pku.edu.cn; jplotkin@sas.upenn.edu

https://doi.org/10.1038/s43588-024-00621-8

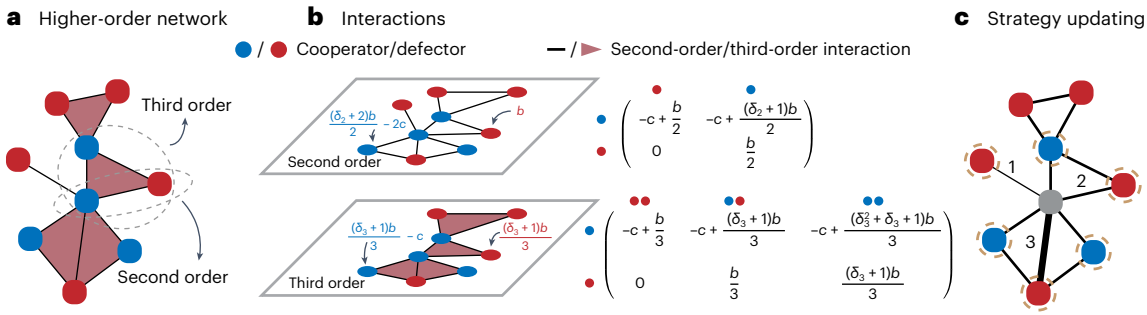

Fig. 1 | Evolutionary dynamics with higher-order interactions. a, The population structure is described by a higher-order network, where nodes represent individuals, edges between nodes (black lines) represent second-order interactions, and three-node closures (shaded triangles) represent third-order interactions. **b**, Every individual adopts a strategy cooperate (blue circles) or defect (red circles) to play nonlinear PGGs in second- and third-order interactions, with payoff matrices shown. An individual obtains payoffs $u^{(2)}$ and $u^{(3)}$ from the two types of interaction, which gives an accumulated payoff $u = u^{(2)} + u^{(3)}$ and associated fitness $F = \exp(\theta u)$. **c**, An individual i (gray node) is randomly selected to update his strategy by imitating one of his interacting partners (brown dashed circles). The probability that i copies j's strategy is proportional to j's fitness F_j and the frequency of interactions involving i and j, indicated by the number along the edges.

interactions can produce a discontinuous transition to an endemic state and a hysteresis loop in a bistable region[36].

A natural question is how higher-order interactions impact the evolutionary dynamics of cooperative behaviors. There is literature that studies multiplayer games in well-mixed populations[21,37,38] or in classical network-structured populations[39–42], although this approach is limited to homogeneous network structures. Another approach is to study linear public goods games (PGGs) on hyper-graphs[43–45]. However, linear PGGs can be resolved into the sum of multiple pairwise games, and they may fail to capture the most interesting, nonlinear effects of higher-order interaction[46].

Here we propose a mathematical model of strategy evolution on arbitrary higher-order networks that captures general multiplayer interactions, including nonlinearity in the outcomes resulting from participants' behaviors. We provide an analytical treatment of cooperation with higher-order interactions, taking account of spatial heterogeneity. Our analysis identifies several classes of higher-order interaction networks that provide an advantage for the spread of cooperation above and beyond the effects of purely pairwise interactions. We also apply this analysis to four empirical networks that feature multiple subcommunities connected by weak links. Our analysis reveals when and how higher-order interactions have an impact on the spread of prosocial behaviors in structured populations.

Results

Model summary

Population structure with higher-order interactions. We consider a population of N individuals, labeled by $\mathcal{N} = \{1, 2, ..., N\}$. Individuals may participate in social interactions of multiple different orders, including, for instance, pairwise and three-way game interactions. A classic pairwise interaction is said to have order two, while a third-order interaction involves a game with simultaneous behavior by three participants. Let an ℓ-element set $[i_1, i_2, ..., i_\ell]$ denote an ℓth-order interaction, with $i_j \in \mathcal{N}$ and $i_j \neq i_k$ for any $j \neq k$. The set for all possible ℓth-order interactions (that is, randomly choosing ℓ different individuals from $\mathcal{N}$) is

$$\mathcal{L}^{(\ell)} = \{[1, 2, ..., \ell], ..., [N - \ell + 1, N - \ell + 2, ..., N]\}, \quad (1)$$

which has size $|\mathcal{L}^{(\ell)}| = \binom{N}{\ell}$. We specify the ℓ-order interactions within a population by an binary matrix of size N-by-$|\mathcal{L}^{(\ell-1)}|$, denoted $W^{(\ell)}$, whose entry in row i and column J represents an ℓth-order interaction involving participant i and $(\ell - 1)$ other participants, denoted by $J = [j_1, j_2, ..., j_{\ell-1}]$. Let $W^{(\ell)}_{ij} = 1$ if such an ℓth-order $[i, J]$ exists in the population, whereas $W^{(\ell)}_{ij} = 0$ otherwise. For convenience, we use the notation $w_{ij} = 1$ (or $w_{ij} = 0$) to indicate the presence (or absence) of interaction $[i, J]$. We describe any combination of higher-order interactions in a population by a set of matrices, $W^{(\ell)}$, for all possible values of ℓ from 2 to N. We additionally assume all interactions are undirected and there are no self-loops for each order of interaction (Methods).

We can often visualize a set of higher-order interactions by a combination of simplices of different dimensions. For example, Fig. 1a illustrates a population structure with second-order interactions (pairwise interactions) shown as black lines connecting pairs of nodes, and also third-order interactions shown as shaded triangles connecting three nodes, also called 2-simplices. In the main text we focus on interactions of orders two and three; we provide general mathematical results for arbitrary orders in Methods.

Strategy evolution in the structured population proceeds by payoff-biased imitation. In each generation, every individual adopts either cooperation (C) or defection (D) to play in all second- and third-order interactions (Fig. 1b). Let x_i denote individual i's strategy, where $x_i = 1$ is cooperation and $x_i = 0$ is defection.

Public goods games. Higher-order interactions take the form of a symmetric PGG, which is a form of social dilemma for $\ell \geq 2$ concurrent players. Cooperators pay a cost c to contribute toward the production of a public benefit, which is divided equally among all ℓ players in the game (whether they cooperated or not). Defectors pay no cost and provide no public benefit. In particular, if n of the players are cooperators and the remaining $(\ell - n)$ players are defectors, then a defector and a cooperator receive respective payoffs

$$\pi_D = \frac{b_n}{\ell}, \qquad \pi_C = \frac{b_n}{\ell} - c, \quad (2)$$

where b_n denotes the total public benefit produced as the result of the n cooperators in the game.

The simplest PGG is linear: if one cooperator alone produces public benefit $b_1 = b$ then, in the linear case, n cooperators produce total benefit $b_n = nb$. But the linear PGG can be treated as a series of pairwise games, and so it fails to capture any interesting effects of higher-order interactions. Therefore, we study nonlinear public goods, such that the additional public good produced by each subsequent cooperator

is not a constant amount. In particular, we consider the following form of nonlinearity[28]:

$$\begin{aligned} b_n &= b\left(1+\delta+\delta^2+\cdots+\delta^{n-1}\right) \\ &= b\frac{1-\delta^n}{1-\delta}, \end{aligned} \tag{3}$$

which has the interpretation that the public benefit produced by each subsequent cooperator is modified by a factor δ, called the benefit factor. The case $\delta = 1$ reduces to the linear PGG. This formulation of nonlinear public goods is motivated by a general principle for the marginal utility of additional contributions to a common pool, namely:

$$B(x+h) - B(x) = \Delta(h)(B(x) - B(x-h)), \tag{4}$$

where $B(x)$ denotes the benefit produced from total contribution x. This equation says that there are marginal returns on additional investment in the public pool, and that the marginal utility of additional contribution h does not depend on the total contribution x to which it is added.

To be completely general, we allow for different nonlinearities in ℓ-player PGGs, when interactions differ in the number of players involved. That is, we allow different benefit factors for second- and third-order social interactions, δ_2 and δ_3 respectively (see Fig. 1b for detailed payoff matrices). Individual i then obtains the following payoffs from second- and third-order PGGs:

$$\begin{aligned} u_i^{(2)} &= \sum_{j\in\mathcal{L}^{(1)}} w_{ij}\left[\left(\frac{b}{2}-c\right)x_i + \frac{b}{2}x_j + \frac{(\delta_2-1)b}{2}x_ix_j\right], \\ u_i^{(3)} &= \sum_{j,k\in\mathcal{L}^{(2)}} w_{ijk}\left[\left(\frac{b}{3}-c\right)x_i + \frac{b}{3}(x_j+x_k)\right. \\ &\quad \left. + \frac{(\delta_3-1)b}{3}(x_ix_j+x_ix_j+x_jx_k) + \frac{(\delta_3-1)^2b}{3}x_ix_jx_k\right]. \end{aligned} \tag{5}$$

Individual i's accumulated payoff across interactions of all orders is then $u_i = u_i^{(2)} + u_i^{(3)}$, which determines i's fitness $F_i = \exp(\theta u_i)$. Here θ ($0 \le \theta < 1$) is called the strength of selection, and it measures how strongly fitness influences the propensity to copy a player's strategy. We focus on the regime of weak selection, $\theta \ll 1$ (ref. 47).

Strategy evolution by payoff-biased imitation. After all interactions occur and payoffs accumulate, a random individual i is selected uniformly to consider changing his or her strategy. Following the widely used death–birth updating rule, individual i imitates a random individual j's strategy with probability proportional to j's fitness F_j and the frequency of interactions involving i and j, given by $r_{ij} = w_{ij} + \sum_{k\in\mathcal{N}} w_{ijk}$ (Fig. 1c). Therefore, the probability that individual i copies j's strategy is given by

$$p_{j\to i} = \frac{1}{N}\frac{F_j r_{ij}}{\sum_{k\in\mathcal{N}} F_k r_{ik}}. \tag{6}$$

Note that strategy updating acts on a so-called replacement graph (that is, location reproduction) with edge weight r_{ij} equal to the total number of interactions occurring on edge (i,j) per unit of time (see equation (16)).

General rule for the evolution of cooperation

In the absence of mutation, the population will eventually reach one of two absorbing states: the all-cooperator state or the all-defector state. We let ρ_C denote the probability that a cooperator, occupying a random node in a population otherwise full of defectors, will eventually spread to the entire population through the process of payoff-biased strategy imitation[48]. We say that selection favors cooperation when the fixation probability is larger than in the absence of selection, namely, $\rho_C > 1/N$.

We have proven that cooperation is favored by natural selection (that is, $\rho_C > 1/N$) when

$$\left(f_b^{(2)} + f_b^{(3)}\right)b - \left(f_c^{(2)} + f_c^{(3)}\right)c > 0, \tag{7}$$

where $f_b^{(\ell)}$ and $f_c^{(\ell)}$ denote the coefficient of benefit b and cost c, arising from ℓth-order interactions. Intuitively, the above condition means that, when a random player is selected to update his strategy, a cooperative neighbor has a higher accumulated payoff from second-order and third-order interactions than a random neighbor. The corresponding threshold benefit-to-cost ratio required for selection to favor cooperation is given by

$$\left(\frac{b}{c}\right)^* = \frac{f_c^{(2)} + f_c^{(3)}}{f_b^{(2)} + f_b^{(3)}}. \tag{8}$$

The quantities $f_b^{(\ell)}$ and $f_c^{(\ell)}$ ($\ell = 2, 3$) can be calculated from the population structure, namely the pairwise interactions $W^{(2)}$ and the third-order interactions $W^{(3)}$, by solving a system of linear equations of size $O(N^{L+1})$, where L is the highest order of interactions, equal to 3 in the cases we study in the main text (Methods).

The main question we study is: when do higher-order interactions promote cooperation relative to only pairwise interactions? In our model, each population structure has a unique critical benefit-to-cost ratio $(b/c)^*$ above which selection will favor cooperation. When the critical ratio $(b/c)^*$ is smaller (but positive), this indicates that it is easier to promote cooperation. Therefore, we analyze when the critical ratio for a population structure with both second- and third-order interactions, $(b/c)^*_{(2,3)}$, is lower than the critical ratio in a population structure restricted to only pairwise interactions, $(b/c)^*_{(2)}$.

Well-mixed population structures

We first consider a well-mixed population structure. In the case of pairwise interactions alone, when every node in the population of size N is connected to every other node, the critical ratio required to support cooperation is given by

$$\left(\frac{b}{c}\right)^*_{(2)} = \frac{6(N-1)}{(\delta_2+2)(N-2)}. \tag{9}$$

By contrast, if all triplets of nodes are engaged in third-order interactions then the critical ratio for cooperation is given by

$$\left(\frac{b}{c}\right)^*_{(3)} = \frac{18(N-1)}{(\delta_3^2+2\delta_3+3)(N-3)}. \tag{10}$$

Finally, if a population structure includes both all second-order and all third-order interactions then the resulting critical ratio for the hybrid structure is

$$\left(\frac{b}{c}\right)^*_{(2,3)} = \frac{18(N-1)N}{(N-2)\left(6\delta_2+\delta_3^2(N-3)+2\delta_3(N-3)+3(N+1)\right)}. \tag{11}$$

Equations (9)–(11) recover well-known outcomes in a well-mixed population, previously derived using the Moran process[49].

The replacement graphs for well-mixed structures of arbitrary order are all equivalent to that of an unweighted well-mixed population structure: that is, any node can potentially imitate any other node's strategy. Nonetheless, the critical ratio required to favor cooperation in a well-mixed second-order network differs from the ratio in a well-mixed third-order structure. For example, in the simple case of a linear PGG, $\delta_2 = \delta_3 = 1$, the critical ratio is always larger under only third-order interactions, compared with a population with only second-order interactions (Fig. 2a), which reflects a well-known

https://doi.org/10.1038/s43588-024-00621-8

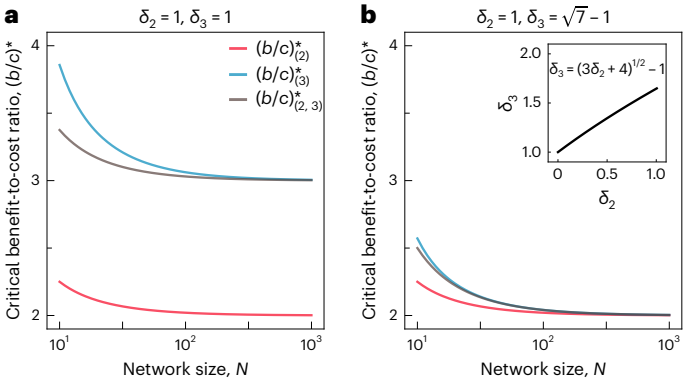

Fig. 2 | The evolution of cooperative behavior depends on the number of players in PGGs and the strength of nonlinearity in their contributions. We plot the critical benefit-to-cost ratio required for the evolution of cooperation, $(b/c)^*$, for well-mixed populations with second-order interactions, third-order interactions, or both second- and third-order interactions. **a**, When all PGGs are linear ($\delta_2 = \delta_3 = 1$), the critical ratio for pairwise interactions (red line) is much lower than that for purely third-order (blue line) or for second- and third-order (brown line) interactions. A larger benefit–cost ratio is required for cooperation when games involve more players, because the social dilemma is stronger for linear three-player PGGs. **b**, To ensure a fair comparison between population structures with second- and third-order interactions, we enforce a relationship between the benefit factors δ_2 and δ_3 (inset), such that resulting social dilemma is identical for pairwise and three-player games, in the limit of a large well-mixed population. The plot shows the critical ratio for second-order benefit factor $\delta_2 = 1$ and corresponding third-order factor $\delta_3 = \sqrt{7} - 1$. When enforcing this relationship the critical ratios for cooperation all converge to 2 as the population size N gets large.

effect of group size[37]. There is a simple intuition for this result. The total benefit produced in each PGG is divided equally among all players involved in the interaction—and so the social dilemma is more acute for third-order interactions than for second-order interactions (with $\delta_2 = \delta_3$), leading to a larger benefit-to-cost ratio required to favor cooperation for third-order interactions.

We are interested in the effects of higher-order interactions compared with pairwise interactions. But the results in Fig. 2a show that, to make a fair comparison between second- and third-order interactions, we must introduce a stronger nonlinearity in the three-player PGGs than in the two-player games. In other words, we must ensure the marginal public benefit from each additional cooperator is larger in the three-player game than in the two-player game. The principle we follow is to choose δ_3 as a function of δ_2 such that the critical ratios for well-mixed populations of second- and third-order interactions will be the same, at least in the limit of $N \to \infty$. We can solve for this relationship between benefit factors:

$$\delta_3 = (3\delta_2 + 4)^{1/2} - 1. \tag{12}$$

The effect of enforcing this relationship is shown in Fig. 2b. As desired, when enforcing this relationship, the critical ratios for second-order and third-order well-mixed populations are the same, in the limit of large population $N \to \infty$, so that comparisons between interactions of different orders are now fair. (Moreover, when N is finite, the critical benefit-to-cost ratio for third-order interactions is always larger than for second-order interactions—which is a conservative result when studying whether higher-order interactions facilitate cooperation.)

We will enforce the relationship above between the benefit factors δ_3 and δ_2 (equation (12)) throughout our analysis, so that higher-order interactions (or a mixture of second-order and higher-order interactions) are always compared on a fair basis with strictly second-order interactions. We will often use two representative examples of equation (12): $(\delta_2, \delta_3) = (0, 1)$ and $(\delta_2, \delta_3) = (1, \sqrt{7} - 1)$. The first example illustrates that a two-player threshold PGG is equivalent, from the perspective of cooperation in an infinitely large well-mixed population, to a three-player linear PGG.

By construction, when we compare higher-order interactions to pairwise interactions on a fair basis (enforcing equation (12)), we find that higher-order interactions never promote the evolution of cooperation in well-mixed populations: that is, $(b/c)^*_{(2)} \leq (b/c)^*_{(3)}$ and $(b/c)^*_2 \leq (b/c)^*_{(2,3)}$ in well-mixed populations. The question still remains, though, whether higher-order interactions might facilitate cooperation, by lowering the required benefit–to-cost ratio, in populations with non-trivial structures.

Higher-order star networks

We use star networks as the first type of non-trivial population structure, to study the impact of higher-order interactions on the evolution of cooperation. It is already well known that star networks facilitate cooperation in the context of pairwise interactions alone[10]. Here we ask whether including higher-order interactions into such structures will have any additional effect on the evolution of cooperative behavior.

A higher-order star network is defined by a single root node with m branches. Each branch contains two leaf nodes connected with each other and with the root, so there are a total of $N = 2m + 1$ individuals in the population and $3m$ edges. If we allow for third-order interactions as well, then we add m 2-simplices, each involving the root node and the two leaf nodes of a branch (Fig. 3a)

All individuals are connected by purely third-order interactions in the star network, and so ρ_C and $(b/c)^*$ are well defined even when the structure contains only third-order interactions. In addition, the replacement graphs are also equivalent under second- and third-order interactions, so that $(b/c)^*_{(2,3)}$ will always fall between $(b/c)^*_{(2)}$ and $(b/c)^*_{(3)}$.

We have derived analytic expressions for the critical ratio that favors cooperation on higher-order star networks (Supplementary Section 3). Enforcing equation (12), to make a fair comparison between second- and third-order structures, we find that $(b/c)^*_{(2,3)}$ is always lower than $(b/c)^*_{(2)}$, for any number of branches m and any value of δ_2. In other words, including higher-order interactions on the star network always facilitates the evolution of cooperation (Fig. 3c). In the limit of many branches, $m \to \infty$, we have the relatively simple exact expressions

$$\begin{aligned} \left(\frac{b}{c}\right)^*_{(2)} &= \frac{24}{5(\delta_2+2)}, \\ \left(\frac{b}{c}\right)^*_{(2,3)} &= \frac{14364}{3501\delta_2 - 374\sqrt{3\delta_2+4}+7132}, \end{aligned} \tag{13}$$

and the relation $(b/c)^*_{(2,3)} < (b/c)^*_{(2)}$ still holds (Fig. 3d).

Pairwise projection graphs

The effects of higher-order interactions can also be understood using a pairwise projection graph[20,50]. The addition of higher-order interactions provides group-size variation[38,51] and more opportunities for individuals to interact than purely pairwise interactions. Therefore, we would like to determine whether the cooperating-promoting effects of higher-order interactions are caused simply by adding more opportunities for local interactions, or whether it is due to the particular arrangement of higher-order structures—such as the 2-simplices associated with each branch in the higher-order star networks.

To resolve this question, for any given higher-order population structure, we construct a corresponding weighted pairwise projection graph, which has the same topology and weights as the replacement graph of the higher-order network. In other words, the projection graph includes an edge weight for every pair of nodes that is involved

https://doi.org/10.1038/s43588-024-00621-8

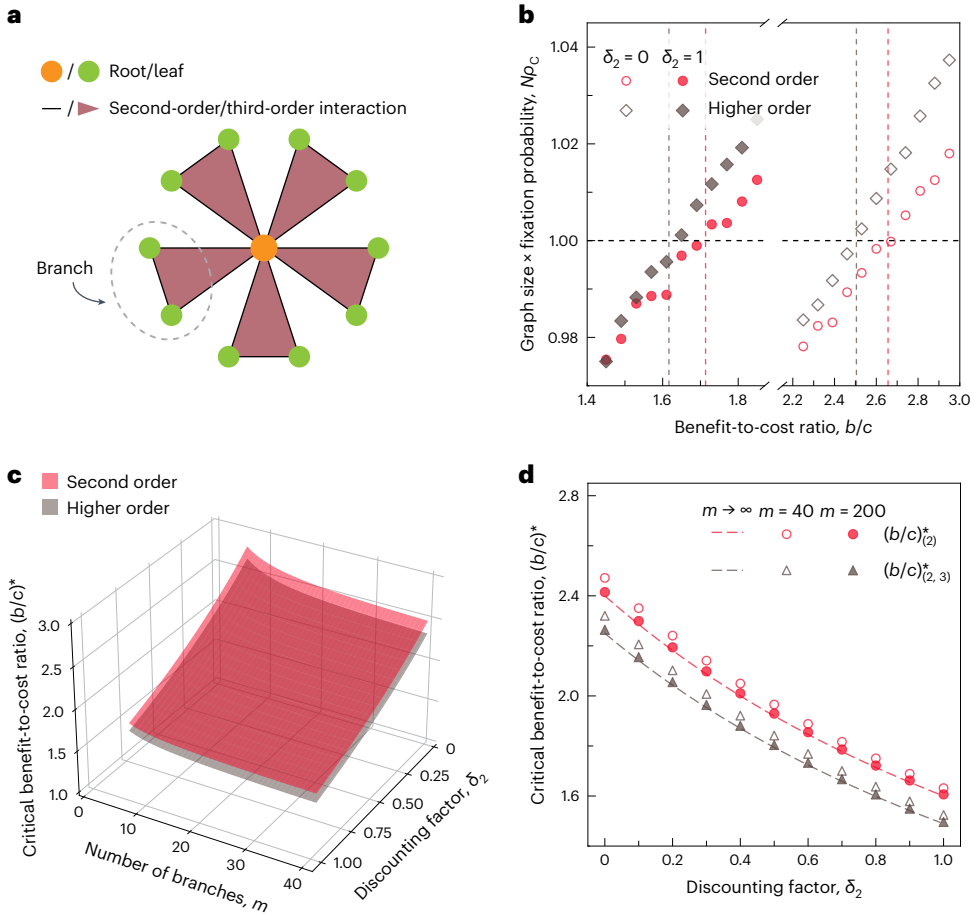

Fig. 3 | Higher-order interactions can facilitate cooperation. We consider a higher-order star network, composed of one root node and m branches. **a**, In the higher-order star network, each branch consists of two leaf nodes and forms a closure triangle with the root. The network size is thus $N = 1 + 2m$. **b**, The rescaled fixation probability of cooperators, Np_C, as a function of the benefit-to-cost ratio b/c in the PGG. Selection favors cooperation if Np_C exceeds the horizontal line, that is $Np_C > 1$. We analyze two different benefit factors, $\delta_2 = 0$ or $\delta_2 = 1$, each with corresponding values of δ_3 (equation (12)). The dots show the results of 10^7 Monte Carlo simulations and the vertical lines show the analytical prediction for the benefit-to-cost ratio $(b/c)^*$ required to favor cooperation. Higher-order introductions (gray) decrease the benefit required to support the evolution of cooperation, compared with strictly pairwise interactions (red). **c**, The benefit-to-cost ratio $(b/c)^*$ required for cooperation to evolve as a function of the number of branches m and the benefit factor δ_2. For all values of m and δ_2, the introduction of higher-order interactions makes it easier for cooperation to evolve. **d**, An explicit analytical result of the benefit-to-cost ratio required for cooperation. The dots correspond to the exact result from equation (8) for finite population sizes and the dashed lines show results in the limit of $m \to \infty$ (equation (13)). We determine the fixation probabilities by the fraction of 10^7 runs where cooperators reach absorption. Parameter values: $c = 1$, $\theta = 0.01$, $m = 10$ (**b**).

in a distinct ℓ-simplex. The resulting weighted projection graph is therefore a pairwise network that has the same number of interactions as in the higher-order structure, and so it serves as a control to test whether effects on evolutionary dynamics are caused merely by extra opportunities for interaction, as opposed to higher-order structures themselves.

In the case of higher-order star structures, the critical ratio of the associated projection network is greater than $(b/c)^*_{(2,3)}$ (Supplementary Fig. 1a), which indicates that higher-order interactions in these structures facilitate cooperation, above and beyond just the addition of more social interactions.

Intuition for the effects of higher-order interactions

To help understand how higher-order interactions facilitate cooperation in star structures, we consider an evolutionary trajectory starting from the initial state with a single cooperator in a leaf node (Fig. 4). We focus on how third-order interactions—PGG games played among two leaf nodes and the center node—increase the prospects for cooperation, compared with pairwise interactions. The spread of the cooperative type to the second leaf node occurs by random drift. However, once both leaves are cooperators, the chance that the center node will imitate a cooperative leaf node is greater for the three-person PGG than for either two-person PGG involving the center node. Therefore, the higher-order structure facilitates the spread of cooperation to the center node. Subsequently, the center node is more likely to resist invasion from a defector leaf node under third-order interactions, than under pairwise games. Once cooperation spreads to a majority of leaves, third-order interactions increase the chance of cooperation spreading further, compared with pairwise games. Therefore, at all steps along the process toward fixation on a star structure, third-order interactions facilitate the spread of cooperation relative to pairwise games.

Multiple-clique population structures

The cooperative benefits of higher-order social interactions are not limited to highly stylized structures such as the star network. There is a broad range of structures that feature multiple cliques of highly connected nodes (called conjoined networks)[52], in which higher-order interactions make it far easier for cooperation to evolve. A multiple-clique network consists of two (or more) sub-graphs connected by pairwise links between them. Each such sub-graph is more dense than the links connecting different sub-graphs.

https://doi.org/10.1038/s43588-024-00621-8

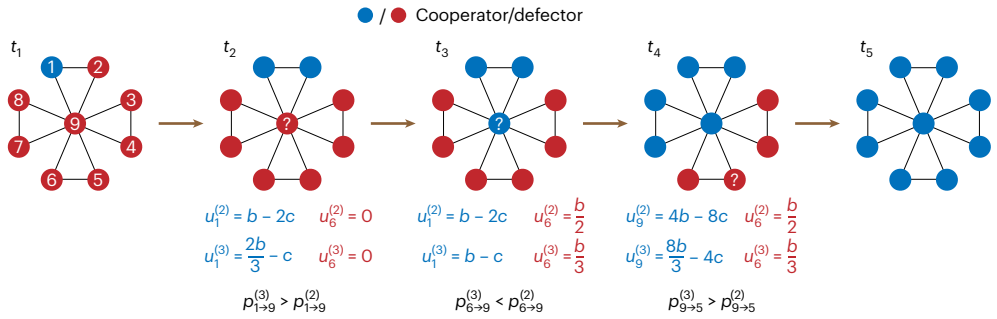

Fig. 4 | Intuition for how higher-order interactions promote cooperation. Higher-order interactions facilitate the spread of cooperation on star structures. We consider an evolutionary process beginning with a single cooperator at a branch node (time t_1). Initially, stochastic drift is responsible for the spread of cooperation from node 1 to node 2, whether under pairwise or third-order interactions. After both leaf nodes are cooperators (time t_2), a leaf cooperator (for instance, node 1) receives payoff $u_1^{(2)}$ and a leaf defector (for instance, node 6) receives payoff $u_6^{(2)}$ under pairwise games; versus payoffs $u_1^{(3)}$ and $u_6^{(3}$ under third-order games. The resulting probability that a cooperator invades the root node (equation (6)) is higher under third-order interactions than under second-order interactions, that is $p_{1\to9}^{(3)} > p_{1\to9}^{(2)}$. In addition, after the root node imitates a cooperator (time t_3), higher-order interactions make it easier for the root to withstand re-invasion by a defector leaf, that is $p_{6\to9}^{(3)} < p_{6\to9}^{(2)}$. Finally, once half of the leaf nodes are cooperators (time t_4), the root node has a greater chance to propagate cooperation to the remaining leaf nodes under third-order interactions than under purely pairwise interactions (for instance, $p_{9\to5}^{(3)} > p_{9\to5}^{(2)}$). Overall, third-order interactions increase the chance that cooperation will eventually fix in the population (time t_5) compared with pairwise interactions. Parameters: $\delta_2 = 0$, $\delta_3 = 1$, $b/c < 3$.

We consider two types of sub-graph: a fully-mixed sub-graph and a 'rich-club' sub-graph. A rich-club network is defined by m_1 central nodes and g peripheral nodes. Each central node is connected to all other nodes, and each peripheral node is connected only to the central nodes. For simplicity, we set $m_1 = 2$ (see Supplementary Section 3 for other cases).

Higher-order interactions do not promote cooperation on a single complete network, or on a single rich-club network. In fact, second-order interactions are more favorable for cooperation on such networks (Supplementary Fig. 2). But when we conjoin two such sub-graphs to each other (that is, one well-mixed sub-graph to another by a single link (Fig. 5a) or one rich club to another by linking their central nodes (Fig. 5d)), then higher-order interactions promote cooperation, by reducing the critical benefit-to-cost ratio required for selection to favor cooperation, relative to pairwise interactions alone.

Even as the number of peripheral nodes g tends to infinity in each sub-graph, $(b/c)^*_{(2,3)}$ is still lower than $(b/c)^*_{(2)}$. Moreover, the effects of higher-order structures in conjoined networks are caused by the higher-order interactions themselves, as opposed to simply an excess of interactions overall—because the corresponding pairwise projection graphs do not show a benefit for cooperation (Supplementary Fig. 1a).

We can analyze the complete network to understand intuitively why multiple-clique higher-order networks promote cooperation (Supplementary Section 4 and Supplementary Fig. 3). Throughout the whole evolutionary process, third-order interactions amplify the difference between the benefit of a cooperator and a random individual two links away. In a single-clique network, a cooperator's benefit is always lower than a random individual's benefit; and so third-order interactions are disadvantageous to cooperation. But in a conjoined two-clique network, the fitness difference is positive, because the average benefit of the random individual is reduced. Third-order interactions extend this advantage, and therefore promote cooperation.

Aside from conjoined complete networks, or conjoined rich-club networks, we systematically analyzed a broad range of multi-clique network structures. We quantify higher-order effects by reporting the difference $(b/c)^*_{(2)} - (b/c)^*_{(2,3)}$—which is positive when higher-order interactions promote cooperation relative to purely second-order interactions, and negative otherwise. Among all 93 structures of size $N = 6$ that have at least one 2-simplex, there are only 6 structures for which higher-order interactions promote cooperation (Extended Data Fig. 1a, red bars). But when we conjoin two such identical structures by adding a single pairwise link, then all 93 resulting two-clique graphs have cooperation facilitated by higher-order interactions (Extended Data Fig. 1a, blue bars). We also calculate the critical ratio of the projection graph for all these two-clique networks, and the results further demonstrate the positive effect of higher-order interactions on cooperation (Supplementary Fig. 1b).

Similar results hold across a broad range of conjoined random networks (random regular, small-world[53] and scale-free networks[54] as shown in Extended Data Fig. 1b and Supplementary Fig. 4). These results suggest that higher-order interactions are generally beneficial for cooperation for population structures with multiple cliques.

Empirical social networks with multiple communities

Empirically measured networks of social interactions frequently feature community structure in their underlying topologies. The density of edges within communities (cliques) is higher than between them. We study four empirical networks from different social contexts: a communication network of 33 women, who were in the role of mothers' club, discussing family planning methods in Korean villages[55]; a friendship network of 34 members in a university karate club for a period of three years from 1970 to 1972, which records interactions between members who communicated outside the club[56]; a social network of 18 women from the Deep South engaging in a set of social events[57], collected in the 1930s; a children's friendship network of 22 fifth-grade students from public elementary schools in a midwestern US community[58]. For each empirical network, we apply Clauset–Newman–Moore greedy modularity maximization[59] to detect community structures (Fig. 6). The number of detected communities is 4, 3, 2 and 2, respectively, and the communities vary in size even within a single network.

We first calculate the critical ratios, $(b/c)^*_{(2)}$ and $(b/c)^*_{(2,3)}$, for each community in isolation. Cooperation is easier to evolve (lower b/c required) under strictly pairwise interactions for all but one community (the purple community in Fig. 6c). But when considering the entire, multi-clique network, we find that higher-order interactions facilitate cooperation in all of these empirical structures.

We also check the cooperation-promoting effect of higher-order interactions under the mutation-selection process, where individuals may accidentally copy the wrong strategy of their neighbors with a specific error rate. We find that the introduction of higher-order interactions can still promote the evolution of cooperation for the entire multi-clique networks even if individuals may make mistakes when updating their behavior (Supplementary Fig. 5).

https://doi.org/10.1038/s43588-024-00621-8

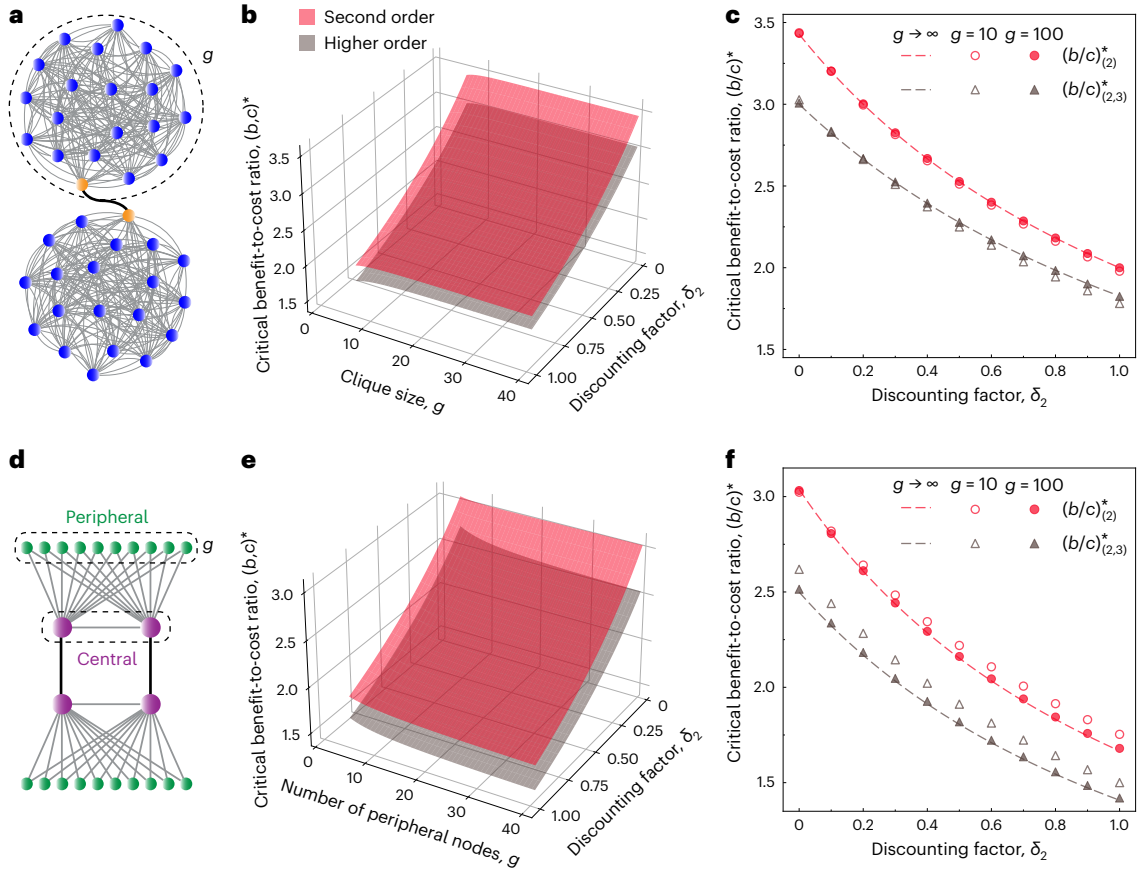

Fig. 5 | Higher-order interactions facilitate cooperation in multi-clique networks. a, A two-clique graph formed by joining two complete sub-graphs graphs of the same size, g. **b**, The critical benefit-to-cost ratio for cooperation as a function of the clique size g and the benefit factor δ_2 for purely pairwise interactions (red plane, $(b/c)^*_{(2)}$) and for the higher-order interactions (gray plane, $(b/c)^*_{(2,3)}$). **c**, Analytical approximations of the benefit-to-cost ratio, for sufficiently large network sizes (lines) and exact analytical computations (dots). Higher-order interactions facilitate cooperation for all network sizes and benefit factors shown. **d**, Two rich-club sub-graphs conjoined by connecting central nodes (purple). Each rich-club graph is composed of two central nodes and g peripheral nodes. Each central node is connected to all other nodes, but the peripheral nodes are only connected to the central nodes. **e**,**f**, Analytical approximations for the critical benefit-to-cost ratio for a finite (**e**) and a infinite (**f**) number of peripheral nodes under second-order or higher-order interactions. In all cases, higher-order interactions facilitate cooperation.

Other pay-off functions

We have analyzed the spread of cooperative behavior in the nonlinear PGG, which is a minimal model of a multiplayer social dilemma. We have assumed a multiplicative nonlinearity in the marginal utility of individual contributions (equation (4)). But other forms of nonlinearity are also reasonable—and we explore two alternative formulations in Supplementary Information (Supplementary Section 5 and Supplementary Figs. 6–8), with similar qualitative results. Although we have developed an analytical treatment for arbitrarily complex interactions, we focused our study on interactions up to the third order, for reasons of computational efficiency. Third-order interactions are sufficient to capture a nonlinear relationship between participants' behaviors, distinct from pairwise interactions.

Our analysis has focused on accumulated payoffs, so that each individual is rewarded by summing their payoffs over all games (pairwise or higher-order) in which they play. An alternative setup is to consider average payoffs—which are normalized, for each individual, by the number of their interactions. We have conducted the same systematic study as in Extended Data Fig. 1 for the uncoupled average payoff and the coupled average payoff (Supplementary Fig. 9), and we find similar results to the case of accumulated payoffs.

Discussion

Population structure has long been recognized as a catalyst for cooperation that cannot otherwise spread in a well-mixed society. The basic mechanism is simple: local interactions promote phenotypic assortment and allow the formation of mutually cooperative partnerships. But human interactions in the real world frequently involve more than two members simultaneously[60–64], and the resulting payoffs are typically nonlinear in the contributions of the interacting individuals[28]. Examples of higher-order interactions range from team collaboration in academia to collective decision-making in human societies[65].

There has been less theoretical research on higher-order interactions than on strictly pairwise interactions[66,67], with some notable exceptions[22–24]. Most techniques for studying multiplayer interactions are limited to homogeneous population structures[22–24]. Unlike pairwise interactions, higher-order interactions may involve different numbers of individuals, making it difficult to analyze all interaction scenarios in heterogeneous populations. Our work provides a systematic way to embrace this complexity, and to analyze the effects of arbitrary population structures that contain interactions of multiple, different orders. We have seen that higher-order interactions often facilitate cooperative behavior above and beyond strictly pairwise interactions in both heterogeneous structures and also homogeneous structures of sufficient size (Supplementary Fig. 10). This effect is especially strong for population structures with several dense cliques connected by weak links between them. We note that these results were obtained under weak selection. Although these results persist in regimes of intermediate selection strength, they may not extend to regimes of strong selection[22,68] (Supplementary Fig. 11).

https://doi.org/10.1038/s43588-024-00621-8

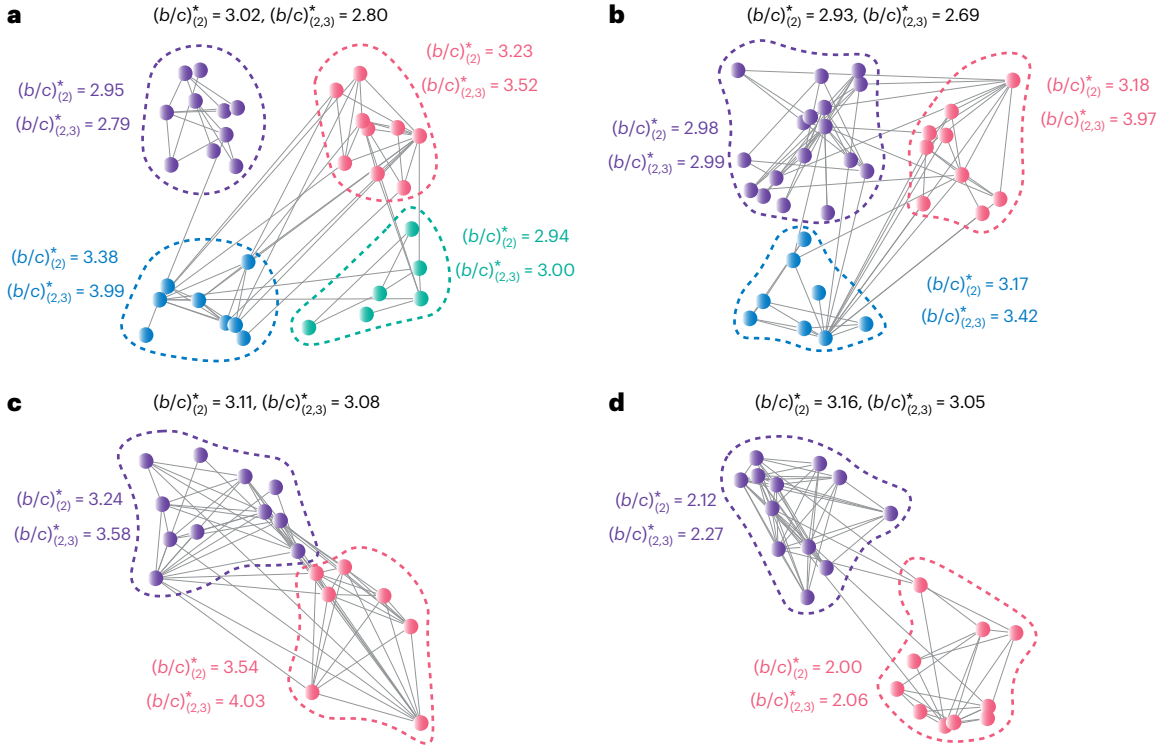

Fig. 6 | Effects of higher-order interactions for empirical social networks. **a**–**d**, We consider four empirical datasets: discussions of family planning among 33 women in Korea[55] (**a**); friendships among 34 members of a university karate club[56] (**b**); social relationships among 18 women[57] (**c**); friendships among 22 fifth-grade students[58] (**d**). We use Clauset–Newman–Moore greedy modularity maximization[59] to identify communities (denoted by nodes of different colors) within each network. We find that $(b/c)^*_{(2,3)}$ exceeds $(b/c)^*_{(2)}$ in almost all communities, individually. But higher-order interactions facilitate cooperation ($(b/c)^*_{(2,3)} < (b/c)^*_{(2)}$) for the entire network, in each of these four empirical examples.

Stylized structures such as the star network help develop an intuition for how, during the course of behavioral imitation, higher-order interactions facilitate the spread of cooperation (Fig. 4). More generally, even for complicated networks with irregular structures, we find that higher-order interactions facilitate cooperation for structures that contain dense sub-networks, or cliques, connected by weak links—including all such examples for cliques of $N = 6$ nodes, as well as a diverse array of random networks with cliques (Extended Data Fig. 1). This finding has relevance to empirical social interactions, because real-world structures often exhibit cliques or communities that can be identified by robust algorithms[69,70]. Community structure is already known to catalyze cooperation in strictly pairwise interactions[52], and here we have shown that these structures promote cooperation more strongly yet, when there are multi-way interactions within each community (Fig. 6). Another way to describe this result is that modularity in network structure predisposes a population to benefit from multi-way interactions. And, indeed, we find that the cooperation-promoting effects of higher-order interactions are strongly correlated with measures of modularity among 3,000 random networks (Supplementary Fig. 12).

In our model, higher-order interactions play an important role in obtaining benefits, but individual behavior is still transmitted through pairwise links. Although pairwise imitation is a natural choice, one possible extension of our model is that higher-order interactions could also act on strategy propagation, where an individual could modulate his choice of neighbor to imitate based on the higher-order structures. A similar idea has been implemented in a generalized epidemic model[36], in which a susceptible node is allowed to be independently infected through different orders of interactions, which produces the expected result that the density of infectious nodes is increasing with additional complex contagion. It is possible that changing the mode of strategy propagation could significantly affect the fate of cooperators—a topic that remains open for future research.

We have provided a mathematical framework to study the evolution of cooperation with arbitrary symmetric games. Nevertheless, there are many related open questions worthy of further study, such as the outcome of temporality[71] and mixing second-order and Nth-order interactions. It is also meaningful to consider evolutionary dynamics in other forms of games, such as the sender–receiver game[72] and asymmetric games[73,74] with a distinct benefit factor in higher-order structures. These remain fertile areas for future investigation on higher-order strategic interactions.

Methods

Here we briefly outline our mathematical analysis for arbitrary higher-order networks, and we refer to Supplementary Information for detailed derivations. We follow the notation developed in 'Results'.

Fixation probabilities for arbitrary higher-order networks

We first introduce the assumptions of our adjacent matrix $W^{(\ell)}$: (1) $w_{i,j}$ equals 0 or 1 (that is, unweighted); (2) for any permutation σ of $[i, j_1, \ldots, j_{\ell-1}]$, $w_{ij_1\ldots j_{\ell-1}} = w_{\sigma(i)\sigma(j_1)\ldots\sigma(j_{\ell-1})}$ (that is, undirected); (3) if any two indexes in $[i, j_1, \ldots, j_{\ell-1}]$ are equal, $w_{ij} = 0$ (that is, no self-loops). The general form of a symmetric ℓ-player game is described by

$$\begin{array}{c} n_C \\ r_C \\ r_D \end{array} \begin{pmatrix} 0 & 1 & \ldots & \ell-1 \\ a_0^{(\ell)} & a_1^{(\ell)} & \ldots & a_{\ell-1}^{(\ell)} \\ b_0^{(\ell)} & b_1^{(\ell)} & \ldots & b_{\ell-1}^{(\ell)} \end{pmatrix},$$

where n_C represents the number of cooperative opponents, and r_C (r_D) represents the payoff of the focal player being a cooperator

(defector). The payoff of i on ℓth-order interactions is denoted as $u_i^{(\ell)}$

$$u_i^{(\ell)} = \sum_{J=(j_1,\ldots,j_{\ell-1})\in\mathcal{L}^{(\ell-1)}} w_{ij} \sum_{(k_1,\ldots,k_\ell)\in\{0,1\}^\ell} v(k_1,\ldots,k_\ell) x_i^{k_1} x_{j_1}^{k_2} \ldots x_{j_{\ell-1}}^{k_\ell}, \quad (14)$$

and individual i's total payoff is the sum of the payoff on each order, given by

$$u_i = u_i^{(2)} + \ldots + u_i^{(L)} = \sum_{I\in\mathcal{L}} c_I^{(i)} x_I, \quad (15)$$

where $\mathcal{L} = \bigcup_{\ell=1}^{L} \mathcal{L}^{(\ell)} \cup \varnothing$, and $v(k_1, \ldots, k_\ell)$ and $c_I^{(i)}$ are the coefficients of $x_i^{k_1} x_{j_1}^{k_2} \ldots x_{j_{\ell-1}}^{k_\ell}$ and x_I, respectively (see Supplementary Information for the explicit mathematical expressions).

For the replacement graph, the weight of edge (i, j) is given by

$$r_{ij} = \sum_{s=1}^{L-1} \sum_{J\in\mathcal{L}^{(s)}, J\ni j} w_{iJ}, \quad (16)$$

the reproductive value of i is $\pi_i = \sum_j r_{ij} / \sum_{i,j} r_{ij}$, and the probability of k-step random walk from i to j is denoted as $p_{ij}^{(k)}$. Then the fixation probability for cooperation is given by the general expression

$$\rho_C = \frac{1}{N} + \frac{\theta}{N}\left(\Lambda_{(2)} - \Lambda_{(0)}\right) + O(\theta^2), \quad (17)$$

where $\Lambda^{(k)} = \sum_{I\in\mathcal{L}} \sum_{j,m=1}^{N} \pi_j c_I^{(m)} p_{jm}^{(k)} \eta_{\{j\}\cup I}$, and for a fixed $I = (i_1, \ldots, i_\ell)$, the following system of linear equations holds for η_I

$$\eta_I = \begin{cases} \frac{1}{\ell} + \frac{1}{\ell} \sum_{y\in\mathcal{N}} \left(p_{i_1 y}^{(1)} \eta_{y,\ldots,i_\ell} + \ldots + p_{i_\ell y^{(1)} \eta_{i_1},\ldots,y} \right) & 2 \le |I| \le L+1, \\ 0 & |I| = 1, \end{cases} \quad (18)$$

Critical ratio under higher-order interactions

For the PGG defined by equation (3), we have the following expansion for ρ_C under weak selection

$$\rho_C = \frac{1}{N} + \frac{\theta}{N}\left[\left(f_b^{(2)} + f_b^{(3)} \right) b - \left(f_c^{(2)} + f_c^{(3)} \right) c \right] + O(\theta^2), \quad (19)$$

and the critical benefit-to-cost ratio under hybrid-order interactions is $(b/c)^*_{(2,3)} = (f_c^{(2)} + f_c^{(3)})/(f_b^{(2)} + f_b^{(3)})$, where $f_c^{(\ell)}$ and $f_b^{(\ell)}$ only depend on ℓth-order interactions, given by

$$\begin{aligned}
f_c^{(2)} &= \sum_{j,m\in\mathcal{N}} \pi_j t_m^{(2)} (p_{jm}^{(2)} - p_{jm}^{(0)}) \eta_{jm}, \\
f_c^{(3)} &= \sum_{j,m\in\mathcal{N}} \pi_j t_m^{(3)} (p_{jm}^{(2)} - p_{jm}^{(0)}) \eta_{jm}, \\
f_b^{(2)} &= \sum_{j,m\in\mathcal{N}} \pi_j \frac{t_m^{(2)}}{2} (p_{jm}^{(2)} - p_{jm}^{(0)}) \eta_{jm} \\
&\quad + \sum_{j,m,j_1\in\mathcal{N}} \pi_j \frac{t_{mj_1}^{(2)}}{2} (p_{jm}^{(2)} - p_{jm}^{(0)}) \eta_{jj_1} \\
&\quad + \sum_{j,m,j_1\in\mathcal{N}} \pi_j \frac{(\delta_2 - 1) t_{m,j_1}^{(2)}}{2} (p_{jm}^{(2)} - p_{jm}^{(0)}) \eta_{jmj_1}, \\
f_b^{(3)} &= \sum_{j,m\in\mathcal{N}} \pi_j \frac{t_m^{(3)}}{3} (p_{jm}^{(2)} - p_{jm}^{(0)}) \eta_{jm} \\
&\quad + \sum_{j,m,j_1\in\mathcal{N}} \pi_j \frac{t_{mj_1}^{(3)}}{3} (p_{jm}^{(2)} - p_{jm}^{(0)}) \eta_{jj_1} \\
&\quad + \sum_{j,m,j_1\in\mathcal{N}} \pi_j \frac{(\delta_3 - 1) t_{mj_1}^{(3)}}{3} (p_{jm}^{(2)} - p_{jm}^{(0)}) \eta_{jmj_1} \\
&\quad + \sum_{j,m,j_1 j_2\in\mathcal{N}} \pi_j \frac{(\delta_3 - 1) t_{mj_1 j_2}^{(3)}}{6} (p_{jm}^{(2)} - p_{jm}^{(0)}) \eta_{jj_1 j_2} \\
&\quad + \sum_{j,m,j_1 j_2\in\mathcal{N}} \pi_j \frac{(\delta_3 - 1)^2 t_{mj_1 j_2}^{(3)}}{6} (p_{jm}^{(2)} - p_{jm}^{(0)}) \eta_{jmj_1 j_2},
\end{aligned} \quad (20)$$

and the parameter $t_{i,i_1,\ldots,i_{n-1}}^{(n+m)}$ satisfies

$$t_{ii_1,\ldots i_{n-1}}^{(n+m)} := \sum_{\substack{(j_1,\ldots,j_{n+m-1})\in\mathcal{L}^{(n+m-1)} \\ \{i_1,\ldots,i_{n-1}\}\subset\{j_1,\ldots,j_{n+m-1}\}}} w_{ij_1,\ldots j_{n+m-1}} m \ge 0. \quad (21)$$

In particular, when a population with purely ℓth-order interactions is connected, the corresponding critical ratio is then well defined and given by $(b/c)^*_{(\ell)} = f_c^{(\ell)} / f_b^{(\ell)}$.

Reporting summary

Further information on research design is available in the Nature Portfolio Reporting Summary linked to this article.

Data availability

All empirical network datasets used in this paper are freely and publicly available at https://icon.colorado.edu/#!/networks (see refs. 55–58). Source data are provided with this paper.

Code availability

All numerical calculations were performed in MATLAB R2023a. All data analysis were performed in Python 3.10. All computer code developed in this study has been deposited into a publicly available GitHub repository at https://github.com/anzhisheng/Higher-order-interactions (ref. 75).

References

1. Bavel, JayJ. Van et al. Using social and behavioural science to support COVID-19 pandemic response. *Nat. Hum. Behav.* **4**, 460–471 (2020).
2. Jacquet, J. et al. Intra-and intergenerational discounting in the climate game. *Nat. Clim. Change* **3**, 1025–1028 (2013).
3. Tilman, A. R., Plotkin, J. B. & Akçay, E. Evolutionary games with environmental feedbacks. *Nat. Commun.* **11**, 915 (2020).
4. Perc, Matjaž. et al. Statistical physics of human cooperation. *Phys. Rep.* **687**, 1–51 (2017).
5. Nowak, M. A. & May, R. M. Evolutionary games and spatial chaos. *Nature* **359**, 826–829 (1992).
6. Santos, F. C. & Pacheco, J. M. Scale-free networks provide a unifying framework for the emergence of cooperation. *Phys. Rev. Lett.* **95**, 098104 (2005).
7. Nowak, M. A. Five rules for the evolution of cooperation. *Science* **314**, 1560–1563 (2006).
8. Ohtsuki, H., Hauert, C., Lieberman, E. & Nowak, M. A. A simple rule for the evolution of cooperation on graphs and social networks. *Nature* **441**, 502–505 (2006).
9. Lehmann, L., Keller, L. & Sumpter, DavidJ. T. The evolution of helping and harming on graphs: the return of the inclusive fitness effect. *J. Evol. Biol.* **20**, 2284–2295 (2007).
10. Allen, B. et al. Evolutionary dynamics on any population structure. *Nature* **544**, 227–230 (2017).
11. Nowak, M. A., Sasaki, A., Taylor, C. & Fudenberg, D. Emergence of cooperation and evolutionary stability in finite populations. *Nature* **428**, 646–650 (2004).
12. Taylor, P. D., Day, T. & Wild, G. Evolution of cooperation in a finite homogeneous graph. *Nature* **447**, 469–472 (2007).
13. Tarnita, C. E., Ohtsuki, H., Antal, T., Fu, F. & Nowak, M. A. Strategy selection in structured populations. *J. Theor. Biol.* **259**, 570–581 (2009).
14. Su, Q., Allen, B. & Plotkin, J. B. Evolution of cooperation with asymmetric social interactions. *Proc. Natl Acad. Sci. USA* **119**, e2113468118 (2022).
15. Sheng, A., Li, A. & Wang, L. Evolutionary dynamics on sequential temporal networks. *PLoS Comput. Biol.* **19**, e1011333 (2023).

16. Xia, C., Wang, J., Perc, Matjaž. & Wang, Z. Reputation and reciprocity. *Phys. Life Rev.* **46**, 8–45 (2023).
17. Rousset, François & Billiard, S. A theoretical basis for measures of kin selection in subdivided populations: finite populations and localized dispersal. *J. Evol. Biol.* **13**, 814–825 (2000).
18. Rousset, F. *Genetic Structure and Selection in Subdivided Populations* Vol. 40 (Princeton Univ. Press, 2004).
19. Santos, F. C., Santos, M. D. & Pacheco, J. M. Social diversity promotes the emergence of cooperation in public goods games. *Nature* **454**, 213–216 (2008).
20. Perc, Matjaž., Gómez-Gardenes, Jesús, Szolnoki, A., Floría, L. M. & Moreno, Y. Evolutionary dynamics of group interactions on structured populations: a review. *J. R. Soc. Interface* **10**, 20120997 (2013).
21. Gokhale, C. S. & Traulsen, A. Evolutionary multiplayer games. *Dyn. Games Appl.* **4**, 468–488 (2014).
22. Mullon, C. & Lehmann, L. The robustness of the weak selection approximation for the evolution of altruism against strong selection. *J. Evol. Biol.* **27**, 2272–2282 (2014).
23. Peña, J., Nöldeke, G. & Lehmann, L. Evolutionary dynamics of collective action in spatially structured populations. *J. Theor. Biol.* **382**, 122–136 (2015).
24. Van Cleve, J. Social evolution and genetic interactions in the short and long term. *Theor. Popul. Biol.* **103**, 2–26 (2015).
25. Benson, A. R., Gleich, D. F. & Leskovec, J. Higher-order organization of complex networks. *Science* **353**, 163–166 (2016).
26. Battiston, F. et al. Networks beyond pairwise interactions: structure and dynamics. *Phys. Rep.* **874**, 1–92 (2020).
27. Battiston, F. et al. The physics of higher-order interactions in complex systems. *Nat. Phys.* **17**, 1093–1098 (2021).
28. Hauert, C., Michor, F., Nowak, M. A. & Doebeli, M. Synergy and discounting of cooperation in social dilemmas. *J. Theor. Biol.* **239**, 195–202 (2006).
29. Peña, J. & Nöldeke, G. Cooperative dilemmas with binary actions and multiple players. *Dyn. Games Appl.* **13**, 1156–1193 (2023).
30. Levine, J. M., Bascompte, J., Adler, P. B. & Allesina, S. Beyond pairwise mechanisms of species coexistence in complex communities. *Nature* **546**, 56–64 (2017).
31. Benson, A. R., Abebe, R., Schaub, M. T., Jadbabaie, A. & Kleinberg, J. Simplicial closure and higher-order link prediction. *Proc. Natl Acad. Sci. USA* **115**, E11221–E11230 (2018).
32. Ganmor, E., Segev, R. & Schneidman, E. Sparse low-order interaction network underlies a highly correlated and learnable neural population code. *Proc. Natl Acad. Sci. USA* **108**, 9679–9684 (2011).
33. Milojević, Staša Principles of scientific research team formation and evolution. *Proc. Natl Acad. Sci. USA* **111**, 3984–3989 (2014).
34. Gambuzza, L. V. et al. Stability of synchronization in simplicial complexes. *Nat. Commun.* **12**, 1255 (2021).
35. Grilli, J., Barabás, György, Michalska-Smith, M. J. & Allesina, S. Higher-order interactions stabilize dynamics in competitive network models. *Nature* **548**, 210–213 (2017).
36. Iacopini, I., Petri, G., Barrat, A. & Latora, V. Simplicial models of social contagion. *Nat. Commun.* **10**, 2485 (2019).
37. Peña, J. & Nöldeke, G. Group size effects in social evolution. *J. Theor. Biol.* **457**, 211–220 (2018).
38. Peña, J. Group-size diversity in public goods games. *Evolution* **66**, 623–636 (2012).
39. Peña, J., Wu, B., Arranz, J. & Traulsen, A. Evolutionary games of multiplayer cooperation on graphs. *PLoS Comput. Biol.* **12**, e1005059 (2016).
40. Li, A., Broom, M., Du, J. & Wang, L. Evolutionary dynamics of general group interactions in structured populations. *Phys. Rev. E* **93**, 022407 (2016).
41. Su, Q., Zhou, L. & Wang, L. Evolutionary multiplayer games on graphs with edge diversity. *PLoS Comput. Biol.* **15**, e1006947 (2019).
42. Broom, M. & Rychtář, J. A general framework for analysing multiplayer games in networks using territorial interactions as a case study. *J. Theor. Biol.* **302**, 70–80 (2012).
43. Gomez-Gardenes, J., Romance, M., Criado, R., Vilone, D. & Sánchez, A. Evolutionary games defined at the network mesoscale: the public goods game. *Chaos* **21**, 016113 (2011).
44. Peña, J. & Rochat, Y. Bipartite graphs as models of population structures in evolutionary multiplayer games. *PLoS ONE* **7**, e44514–e44514 (2012).
45. Alvarez-Rodriguez, U. et al. Evolutionary dynamics of higher-order interactions in social networks. *Nat. Hum. Behav.* **5**, 586–595 (2021).
46. Su, Q., Li, A., Wang, L. & Stanley, H. E. Spatial reciprocity in the evolution of cooperation. *Proc. R. Soc. B* **286**, 20190041 (2019).
47. Wu, B., Altrock, P. M., Wang, L. & Traulsen, A. Universality of weak selection. *Phys. Rev. E* **82**, 046106 (2010).
48. McAvoy, A. & Allen, B. Fixation probabilities in evolutionary dynamics under weak selection. *J. Math. Biol.* **82**, 14 (2021).
49. Gokhale, C. S. & Traulsen, A. Evolutionary games in the multiverse. *Proc. Natl Acad. Sci. USA* **107**, 5500–5504 (2010).
50. Liu, R. & Masuda, N. Fixation dynamics on hypergraphs. *PLoS Comput. Biol.* **19**, e1011494 (2023).
51. Peña, J. & Nöldeke, G. Variability in group size and the evolution of collective action. *J. Theor. Biol.* **389**, 72–82 (2016).
52. Fotouhi, B., Momeni, N., Allen, B. & Nowak, M. A. Conjoining uncooperative societies facilitates evolution of cooperation. *Nat. Hum. Behav.* **2**, 492–499 (2018).
53. Watts, D. J. & Strogatz, S. H. Collective dynamics of 'small-world' networks. *Nature* **393**, 440–442 (1998).
54. Barabási, Albert-L. ászló & Albert, R. éka Emergence of scaling in random networks. *Science* **286**, 509–512 (1999).
55. Rogers, E. M. & Kincaid, D. L. *Communication Networks: toward A New Paradigm for Research* (Free Press, 1981).
56. Zachary, W. W. An information flow model for conflict and fission in small groups. *J. Anthropol. Res.* **33**, 452–473 (1977).
57. Davis, A., Gardner, B. B. & Gardner, M. R. *Deep South: A Social Anthropological Study of Caste and Class* (Univ. South Carolina Press, 2009).
58. Anderson, C. J., Wasserman, S. & Crouch, B. A p* primer: logit models for social networks. *Soc. Netw.* **21**, 37–66 (1999).
59. Clauset, A., Newman, MarkE. J. & Moore, C. Finding community structure in very large networks. *Phys. Rev. E* **70**, 066111 (2004).
60. Wang, J., Fu, F., Wu, T. & Wang, L. Emergence of social cooperation in threshold public goods games with collective risk. *Phys. Rev. E* **80**, 016101 (2009).
61. Wu, T., Fu, F. & Wang, L. Partner selections in public goods games with constant group size. *Phys. Rev. E* **80**, 026121 (2009).
62. Szabó, György & Hauert, C. Phase transitions and volunteering in spatial public goods games. *Phys. Rev. Lett.* **89**, 118101 (2002).
63. Szolnoki, A. & Perc, Matjaž. Group-size effects on the evolution of cooperation in the spatial public goods game. *Phys. Rev. E* **84**, 047102 (2011).
64. Souza, M. O., Pacheco, J. M. & Santos, F. C. Evolution of cooperation under *n*-person snowdrift games. *J. Theor. Biol.* **260**, 581–588 (2009).
65. Civilini, A., Anbarci, N. & Latora, V. Evolutionary game model of group choice dilemmas on hypergraphs. *Phys. Rev. Lett.* **127**, 268301 (2021).
66. Allen, B., Lippner, G. & Nowak, M. A. Evolutionary games on isothermal graphs. *Nat. Commun.* **10**, 5107 (2019).
67. McAvoy, A. & Wakeley, J. Evaluating the structure-coefficient theorem of evolutionary game theory. *Proc. Natl Acad. Sci. USA* **119**, e2119656119 (2022).

68. Wu, B., García, Julián, Hauert, C. & Traulsen, A. Extrapolating weak selection in evolutionary games. *PLoS Comput. Biol.* **9**, e1003381 (2013).
69. Fortunato, S. Community detection in graphs. *Phys. Rep.* **486**, 75–174 (2010).
70. Fortunato, S. & Hric, D. Community detection in networks: a user guide. *Phys. Rep.* **659**, 1–44 (2016).
71. Sheng, A., Su, Q., Li, A., Wang, L. & Plotkin, J. B. Constructing temporal networks with bursty activity patterns. *Nat. Commun.* **14**, 7311 (2023).
72. Kumar, A., Chowdhary, S., Capraro, V. & Perc, Matjaž. Evolution of honesty in higher-order social networks. *Phys. Rev. E* **104**, 054308 (2021).
73. McAvoy, A. & Hauert, C. Asymmetric evolutionary games. *PLoS Comput. Biol.* **11**, e1004349 (2015).
74. McAvoy, A., Allen, B. & Nowak, M. A. Social goods dilemmas in heterogeneous societies. *Nat. Hum. Behav.* **4**, 819–831 (2020).
75. Initial release of code for research paper 'Strategy evolution on higher-order networks'. *Code Ocean* https://doi.org/10.24433/CO.7059083.v2 (2024).

Acknowledgements

We thank A. McAvoy for useful comments and discussions. A.S. acknowledges support from the China Scholarship Council (no. 202206010147). Q.S. acknowledges support from Shanghai Pujiang Program (no. 23PJ1405500). L.W. acknowledges support from the National Natural Science Foundation of China (no. 62036002). J.B.P. acknowledges support from the Simons Foundation Math+X grant to the University of Pennsylvania, and from the John Templeton Foundation (grant #62281).

Author contributions

A.S., Q.S., L.W. and J.B.P. conceived the project. A.S. derived analytical results and performed numerical calculations. A.S., Q.S., L.W. and J.B.P. analyzed the data. A.S., Q.S. and J.B.P. wrote the main text with input from L.W. A.S. wrote the Supplementary Information.

Competing interests

The authors declare no competing interests.

Additional information

Extended data is available for this paper at https://doi.org/10.1038/s43588-024-00621-8.

Supplementary information The online version contains supplementary material available at https://doi.org/10.1038/s43588-024-00621-8.

Correspondence and requests for materials should be addressed to Qi Su, Long Wang or Joshua B. Plotkin.

Peer review information *Nature Computational Science* thanks Bin Wu and the other anonymous reviewer(s) for their contribution to the peer review of this work. Primary Handling Editor: Ananya Rastogi, in collaboration with the *Nature Computational Science* team.

https://doi.org/10.1038/s43588-024-00621-8

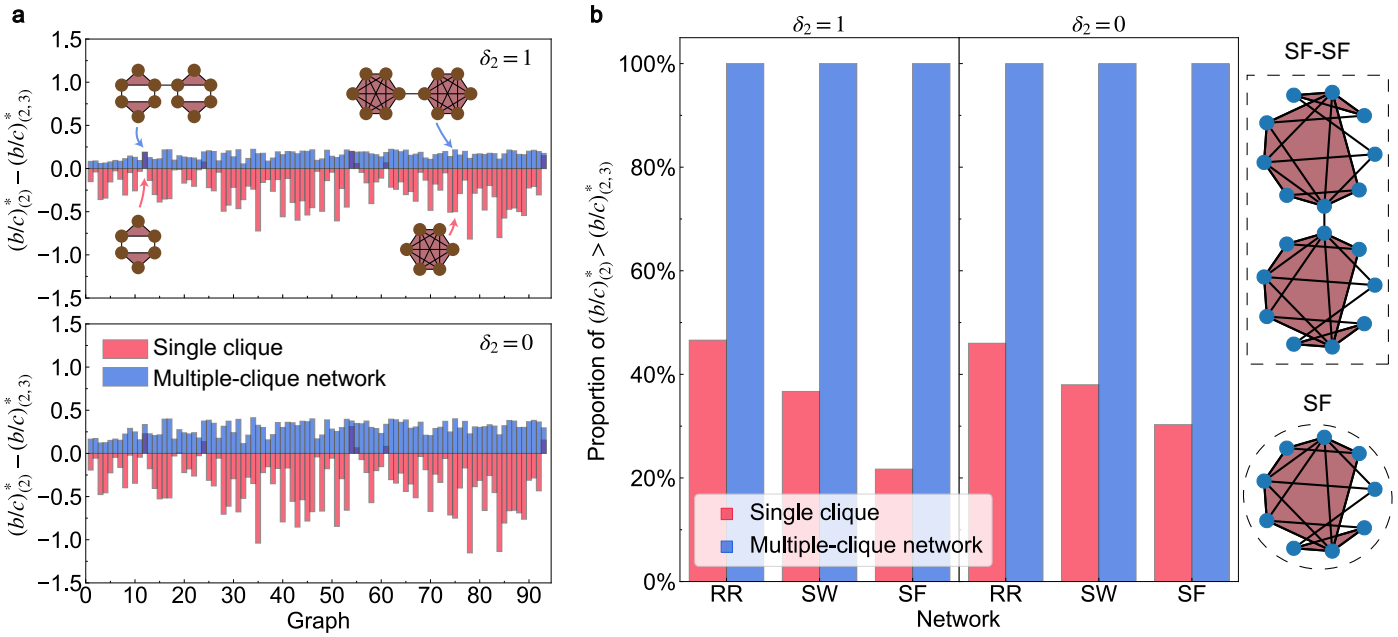

Extended Data Fig. 1 | Evolution of cooperation on a variety of higher-order networks. Cooperation is typically facilitated by higher-order interactions in diverse networks with multiple cliques. **a**, There are 93 networks that have a size of $N = 6$ and contain at least one triangle. Two examples are illustrated in the upper panel. For every single network, the critical benefit-to-cost ratios for purely pairwise interactions $(b/c)^*_{(2)}$ and for higher-order interactions $(b/c)^*_{(2,3)}$ are calculated, and their difference measures how higher-order interactions influence the evolution of cooperation: $(b/c)^*_{(2)} - (b/c)^*_{(2,3)} > 0$ indicates that higher-order interactions facilitate cooperation. For $\delta_2 = 1$ and $\delta_2 = 0$, the red bars show that higher-order interactions facilitate cooperation for only 6 out of the 93 6-node networks. But when we conjoin two such single networks via a random link (averaging over link placement), then higher-order interactions consistently facilitate cooperation (blue bars). **b**, Three representative classes of random networks: random regular networks (RR), Watts-Strogatz small-world networks with rewiring probability $p = 0.3$ (SW)[53], and Barabási-Albert scale-free networks (SF)[54]. For each class, we generated 1,000 networks with size N sampled uniformly from [8, 15] and with average degree sampled in [4,N]. The red bars show the effects of higher-order interactions in these single networks (which facilitate cooperation in less than 50% of cases), whereas the blue bars show the effects of higher-order interactions on two-clique networks generated by connecting two identical networks via the node of highest degree: higher-order interactions facilitate cooperation for all such conjoined networks.

nature portfolio

Corresponding author(s): Joshua B. Plotkin, Long Wang, Qi Su

Last updated by author(s): Feb 29, 2024

Reporting Summary

Nature Portfolio wishes to improve the reproducibility of the work that we publish. This form provides structure for consistency and transparency in reporting. For further information on Nature Portfolio policies, see our Editorial Policies and the Editorial Policy Checklist.

Statistics

For all statistical analyses, confirm that the following items are present in the figure legend, table legend, main text, or Methods section.

n/a	Confirmed
☐	☒ The exact sample size (*n*) for each experimental group/condition, given as a discrete number and unit of measurement
☒	☐ A statement on whether measurements were taken from distinct samples or whether the same sample was measured repeatedly
☒	☐ The statistical test(s) used AND whether they are one- or two-sided *Only common tests should be described solely by name; describe more complex techniques in the Methods section.*
☒	☐ A description of all covariates tested
☒	☐ A description of any assumptions or corrections, such as tests of normality and adjustment for multiple comparisons
☒	☐ A full description of the statistical parameters including central tendency (e.g. means) or other basic estimates (e.g. regression coefficient) AND variation (e.g. standard deviation) or associated estimates of uncertainty (e.g. confidence intervals)
☐	☒ For null hypothesis testing, the test statistic (e.g. *F*, *t*, *r*) with confidence intervals, effect sizes, degrees of freedom and *P* value noted *Give P values as exact values whenever suitable.*
☒	☐ For Bayesian analysis, information on the choice of priors and Markov chain Monte Carlo settings
☒	☐ For hierarchical and complex designs, identification of the appropriate level for tests and full reporting of outcomes
☐	☒ Estimates of effect sizes (e.g. Cohen's *d*, Pearson's *r*), indicating how they were calculated

Our web collection on statistics for biologists contains articles on many of the points above.

Software and code

Policy information about availability of computer code

Data collection	All numerical calculations were performed in Matlab R2023a. All computer code developed in this study has been deposited into the publicly available GitHub repository at https://github.com/anzhisheng/Higher-order-interactions.
Data analysis	All data analysis were performed in Python 3.10.

For manuscripts utilizing custom algorithms or software that are central to the research but not yet described in published literature, software must be made available to editors and reviewers. We strongly encourage code deposition in a community repository (e.g. GitHub). See the Nature Portfolio guidelines for submitting code & software for further information.

Data

Policy information about availability of data

All manuscripts must include a data availability statement. This statement should provide the following information, where applicable:

- Accession codes, unique identifiers, or web links for publicly available datasets
- A description of any restrictions on data availability
- For clinical datasets or third party data, please ensure that the statement adheres to our policy

Source Data for Figures 2, 3, and 5 and Extended Data Figure 1 are available. All the empirical network datasets used in this paper are freely and publicly available at https://icon.colorado.edu/#!/networks.

Human research participants

Policy information about studies involving human research participants and Sex and Gender in Research.

Reporting on sex and gender	N/A
Population characteristics	N/A
Recruitment	N/A
Ethics oversight	N/A

Note that full information on the approval of the study protocol must also be provided in the manuscript.

Field-specific reporting

Please select the one below that is the best fit for your research. If you are not sure, read the appropriate sections before making your selection.

☐ Life sciences ☒ Behavioural & social sciences ☐ Ecological, evolutionary & environmental sciences

For a reference copy of the document with all sections, see nature.com/documents/nr-reporting-summary-flat.pdf

Behavioural & social sciences study design

All studies must disclose on these points even when the disclosure is negative.

Study description	This study is theoretical in nature and is based on analytical calculations (described in Supplementary Information). No empirical data collection were collected for this study.
Research sample	All of the new "data" we analyzed were produced by simulations (see Source Data), as opposed to empirical data. We did, in addition, analyze four empirical datasets describing social interactions collected from different social contexts. The datasets are representative to study real-world human interactions. They are freely and publicly available at https://icon.colorado.edu/#!/networks.
Sampling strategy	The networks we sampled include random regular networks, scale-free networks, and small-world networks, which are regarded as representative in the field of network science and effectively model social interactions. We incorporate various network sizes and average degrees, and we demonstrated that the results remain unchanged when varying the network size and average degree.
Data collection	No data collection was performed in this study.
Timing	No data collection was performed in this study.
Data exclusions	No data were excluded from the analyses.
Non-participation	No participants were involved in this study.
Randomization	Randomization was used in Monte Carlo simulations, including using numpy.random.random() function in Python to generate random numbers between 0 and 1.

Reporting for specific materials, systems and methods

We require information from authors about some types of materials, experimental systems and methods used in many studies. Here, indicate whether each material, system or method listed is relevant to your study. If you are not sure if a list item applies to your research, read the appropriate section before selecting a response.

Materials & experimental systems

n/a	Involved in the study
☒	☐ Antibodies
☒	☐ Eukaryotic cell lines
☒	☐ Palaeontology and archaeology
☒	☐ Animals and other organisms
☒	☐ Clinical data
☒	☐ Dual use research of concern

Methods

n/a	Involved in the study
☒	☐ ChIP-seq
☒	☐ Flow cytometry
☒	☐ MRI-based neuroimaging